

Magnetoelectric coupling in zigzag graphene nanoribbons

J. Jung* and A. H. MacDonald

Department of Physics, University of Texas at Austin, Austin, Texas 78712, USA

(Received 9 April 2010; published 5 May 2010)

Zigzag graphene nanoribbons can have magnetic ground states with ferromagnetic, antiferromagnetic, or canted configurations, depending on carrier density. We show that an electric field directed across the ribbon alters the magnetic state, favoring antiferromagnetic configurations. This property can be used to prepare ribbons with a prescribed spin-orientation on a given edge.

DOI: [10.1103/PhysRevB.81.195408](https://doi.org/10.1103/PhysRevB.81.195408)

PACS number(s): 75.85.+t, 73.20.-r, 73.22.-f, 75.75.-c

I. INTRODUCTION

Expanding techniques that can achieve electrical control of spin is a key goal of both metal and semiconductor spintronics.^{1,2} In metal spintronics, for example, electrical spin-transfer torque³ research seeks to amplify the potential⁴ of technologies based on giant magnetoresistance⁵ and tunnel magnetoresistance.⁶ The aim of research on dilute magnetic semiconductors⁷ is to create semiconductor materials in which magnetic properties are as sensitive to doping and external gate potentials as electrical properties. Recent interest in the spin Hall effect⁸ and the topological magnetoelectric effect⁹ is motivated by a search for effects which enable electrical control of spin in nonmagnetic materials. In this context it is interesting to address the possibility of interesting magnetoelectric effects in graphitic material. The physics of zigzag graphene ribbons and edge terminations has received considerable attention recently.^{10–40} Magnetism is expected in any graphitic material containing ribbon segments with zigzag edge^{10–25} terminations, for example highly defected bulk graphitic material.^{41–43,45} Thanks to progress in structural control of graphene flakes and related materials,⁴⁶ prospects for mastering graphitic magnetism have improved. The perfect zigzag nanoribbon studied in this paper may be viewed as a model system in which graphitic magnetism is exhibited in its simplest and most essential form.

The magnetic ground state of a zigzag nanoribbon has collective moments localized near its edges. In the absence of a transverse electric field, a doped nanoribbon has either full or partial orientational alignment^{47,48} between moments on opposite edges, as illustrated schematically in Fig. 1. We show that an external electric field applied across the ribbon can control the relative orientation angle θ , and that this property can be used to prepare ribbons with a prescribed spin-orientation on a given edge.

II. HUBBARD MODEL MEAN-FIELD THEORY

Since *ab initio* density-functional and simpler model Hamiltonian approaches make essentially identical predictions,^{19,23,24,43} we base our analysis of zigzag-ribbon magnetism on a Hubbard model which allows the underlying physics to be identified more clearly. The success of the Hubbard model has been shown to be due to the essentially local character of edge magnetism in graphene ribbons.⁴⁴ The Hubbard model mean-field Hamiltonian for noncollinear spins,

$$H_{\sigma} = -\gamma_0 \sum_{\langle i,j \rangle} c_{i\sigma}^{\dagger} c_{j\sigma} + \sum_i c_{i\sigma}^{\dagger} c_{i\sigma} (v_{ext} + e\mathcal{E}y_i) + \frac{U}{2} \sum_i [\langle c_{i\sigma}^{\dagger} c_{i\sigma} \rangle c_{is}^{\dagger} c_{is} - \langle c_{i\sigma'}^{\dagger} \vec{\tau}_{\sigma',\sigma} c_{i\sigma} \rangle \cdot c_{is'}^{\dagger} \vec{\tau}_{s',s} c_{is}], \quad (1)$$

has a term which represents hopping between nearest neighbor π -orbitals with amplitude $\gamma_0 = 2.6$ eV, an external potential term which accounts for the transverse electric field, and a mean-field interaction term. We assume sums over repeated indices. The operator $c_{i\sigma}^{\dagger}$ creates a π orbital electron at site i with spin σ , \mathcal{E} is the transversal electric field, y_i is the position of lattice site i along the ribbon width and $\vec{\tau}_{\sigma',\sigma}$ represents the elements of the three Pauli matrixes. As a convenience we include a constant term $v_{ext} = -U$ in the external potential which removes the interaction with a unit charge on each site from the mean-field quasiparticle energy. [All spin indices in Eq. (1) are summed over.] Note that the mean-field interaction energy of an electron on site i is spin dependent and proportional to the density of opposite spin electrons. Following Yazyev *et al.*,⁴³ we choose $U = 3$ eV a value slightly larger than estimates based on the local density ap-

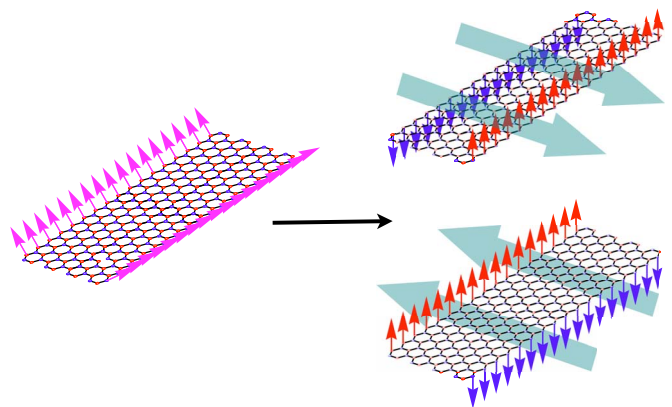


FIG. 1. (Color online) Schematic representation of the influence of a lateral electric field on zigzag-ribbon magnetism. The figure on the left represents the Noncollinear ground state of a doped zigzag ribbon with a canted angle θ between the spin moment orientations on opposite edges. On the right we represent how a lateral electric field represented with large green arrows drives the angle θ to π , an antiferromagnetic configuration similar to that of an undoped ribbon.

proximation used in some previous Hubbard model analyses.^{19,21,48} We have used 1200 k points in the Brillouin zone for the self-consistent calculations. Zigzag edge magnetism is very sensitive⁴⁸ to the net charge density of the ribbon δn , which we refer to as doping whether due to chemical dopants or gate voltages and measure per repeat distance $a=2.46$ Å along the edge. The corresponding areal density is $\delta n_{2D}=\delta n/W$ where the ribbon width $W=\sqrt{3Na}/2$ and N is the number of atom pairs per ribbon unit cell.

III. EDGE ONLY MODEL

The influence of a transverse electric field on electronic structure in neutral ribbons has been studied previously for both armchair⁴⁹ and zigzag cases^{16,50,51} using density-functional theory. The essentials of zigzag-ribbon magnetism and of the transverse-field magnetoelectric effect are captured by an *edge-state-only* model;^{19,21} the qualitative discussion below refers mainly to this model and to the special case of collinear magnetic states ($\theta=0$ or $\theta=\pi$), but the numerical calculations and the phase-diagram results are based on solutions of the full noncollinear π -band Hubbard model self-consistent field equations. In the edge-only model the spin-dependent mean-field Hamiltonian for collinear states^{21,44} takes the form of a two-dimensional matrix for each value of k ,

$$H_\sigma(k) = [\sigma\Delta_z(k) + \Delta_\varepsilon(k)]\tau_z + [\Delta_0(k) + h_z]\sigma I + t(k)\tau_x. \quad (2)$$

Here the τ_α are Pauli matrices which act on the *which edge* degree of freedom. The terms proportional to τ_z in Eq. (2) therefore represent the difference in energy between left ($\tau_z \rightarrow 1$) and right ($\tau_z \rightarrow -1$) edges for electrons of spin σ , whereas the term proportional to τ_x represents the momentum-dependent interedge hopping amplitude. Zigzag edge magnetism follows from the property²¹ that $t(k)$ vanishes rapidly with ribbon width in the part of the Brillouin-zone ($2\pi/3a < |k| < \pi/a$) in which edge states reside. In Eq. (2), $\Delta_z(k)$ captures the difference between exchange energies on opposite edges, which vanishes in the $\theta=0$ (F) state in the absence of a transverse field, whereas $\Delta_0(k)$ captures the spin dependence of the edge average, which vanishes in the $\theta=\pi$ (AF) state. (An irrelevant spin and edge independent exchange energy has been dropped from H_σ). Both exchange energies are large only for the edge-states ($|k| > 2\pi/3a$). h_z accounts for Zeeman coupling to the ribbon spins by an external magnetic field when present.

IV. MAGNETOELECTRIC COUPLING IN UNDOPED RIBBONS

The eigenenergies of the two-dimensional Hamiltonian of Eq. (2) are

$$E_\sigma^\pm(k) = \sigma[\Delta_0(k) + h_z] \pm \sqrt{[\sigma\Delta_z(k) + \Delta_\varepsilon(k)]^2 + t^2(k)}. \quad (3)$$

Note that there are always four distinct eigenvalues in the ferromagnetic case, whereas the antiferromagnetic state bands occur in doubly degenerate pairs when $\Delta_\varepsilon \rightarrow 0$. For undoped ribbons the lowest two edge-states bands are normally fully occupied. In Fig. 2 we plot ribbon band struc-

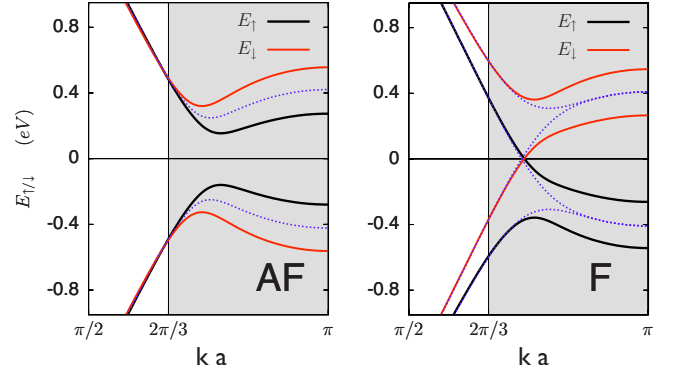


FIG. 2. (Color online) Edge state bands of a zigzag ribbon with $N=20$, nearest-neighbor hopping $\gamma_0=2.6$ eV and on site repulsion $U=3$ eV under a transverse electric field of $\mathcal{E}=0.2$ eV/nm. *Left panel:* In the AF case high-spin (see text) bands shift toward the Fermi energy and the low-spin bands move away. The wave functions of the occupied bands shift density to the low-energy edge. *Right panel:* In the F case Δ_ε shifts the wave vector at which majority and minority spin bands cross to slightly larger values of $|k|$. The dotted lines show the bands at $\Delta_\varepsilon=0$.

tures for both AF and F states of a neutral ribbon calculated using a constant transverse electric field of $\mathcal{E}=0.2$ V/nm. States that are shifted down (up) in energy relative to the $\Delta_\varepsilon=0$ case are localized on the low (high) potential side of the ribbon. (Note that a constant field generates a k dependent Δ_ε because of the k dependence of the degree of edge state localization). In the F-state the Fermi energy is pinned to a band-crossing near $|k|=2\pi/3a$ between the higher energy majority spin band and the lower energy minority spin band. In the AF case we refer to the spin orientation which dominates occupied states on the low (high) potential side of the ribbon as the low-spin (high-spin). (In Fig. 2, \downarrow is the low spin.) A transverse spin shifts the energies of both occupied and unoccupied high-spins toward the Fermi level, lowering the gap. A sufficiently large transverse field will close the indirect gap, creating a half-metallic band structure with only high-spin bands crossing the Fermi level. This is the magnetoelectric effect discussed in earlier^{16,22,51} work. The energy difference between F and AF states²¹ is relatively unchanged by a transverse field. Below we show that in doped ribbons a transverse field tilts the competition between F and AF states in favor of the latter, yielding a distinct and stronger magnetoelectric effect.

V. MAGNETOELECTRIC COUPLING AT FINITE DOPING

We consider for definiteness the case of n -type ribbons in which carriers are added by gate doping. In the absence of a transverse electric field, doping favors^{47,48} the gapless F state over the gapful AF state. The transition between undoped AF and doped F states occurs continuously by varying the relative orientation angle θ between its AF ($\theta=\pi$) and F ($\theta=0$) end points. For small doping densities the magnetization at the edge sites is of the order or $0.25\mu_B$ per lattice constant as can be read from Fig. 5, remaining similar to the values we find for a neutral ribbon. The effect we discuss in this paper

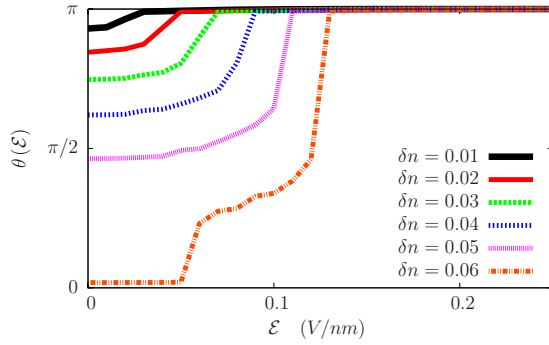


FIG. 3. (Color online) Interedge relative spin orientation angle θ evaluated on the outermost edge atoms as a function of transverse electric field $\Delta_{\mathcal{E}}$ for a series of doping δn values. For $\Delta_{\mathcal{E}}=0$ doping leads immediately to a canting angle $\theta < \pi$ and eventually for δ_n larger than ~ 0.05 to a ferromagnetic state with $\theta=0$. A finite $\Delta_{\mathcal{E}}$ favors the AF state as explained in the text and drives θ toward its undoped value.

is based on the following simple observation concerning the edge-state bands plotted in Fig. 2. In the AF case the conduction band states which are occupied upon doping are high-spin antibonding states, which are localized on the low-energy side of the ribbon. For the F state, on the other hand, there are occupied states in two bands, one localized on the high-energy side and one localized on the low-energy side. The net effect is that a transverse field favors the AF state in doped zigzag ribbons. In Fig. 3 we plot the relative angle between spin polarizations on opposite edges vs lateral electric field for a series of different doping values. These results were obtained by noncollinear spin self-consistent field calculations and confirm the expected magnetoelectric effect. In Fig. 4 we compare the transverse-field dependence of the energy difference between F and AF states for doped and undoped systems. The electric field strength required to convert F states into AF states in doped ribbons is much smaller than the field required to close the AF-state gap in the undoped case. This critical electric field becomes smaller in wider ribbons where the same electric potential difference can be induced with weaker fields. The magnetic anisotropy due to spin orbit terms are very weak in graphene⁵²⁻⁵⁴ and will presumably remain negligibly small in a ribbon. In such

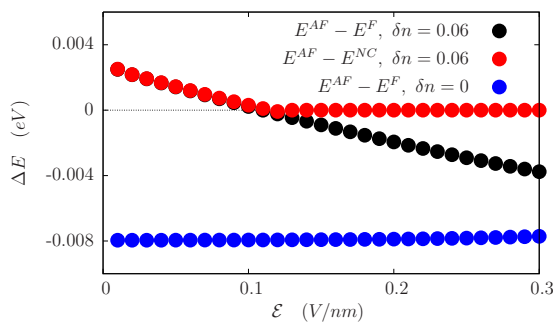


FIG. 4. (Color online) Energy differences (per ribbon unit cell) between the spin collinear AF, F solutions and, for finite-doping, the minimum energy noncollinear (NC) solution. The energy difference between AF and F solutions for $\delta n=0$ has a weak transverse electric field dependence.

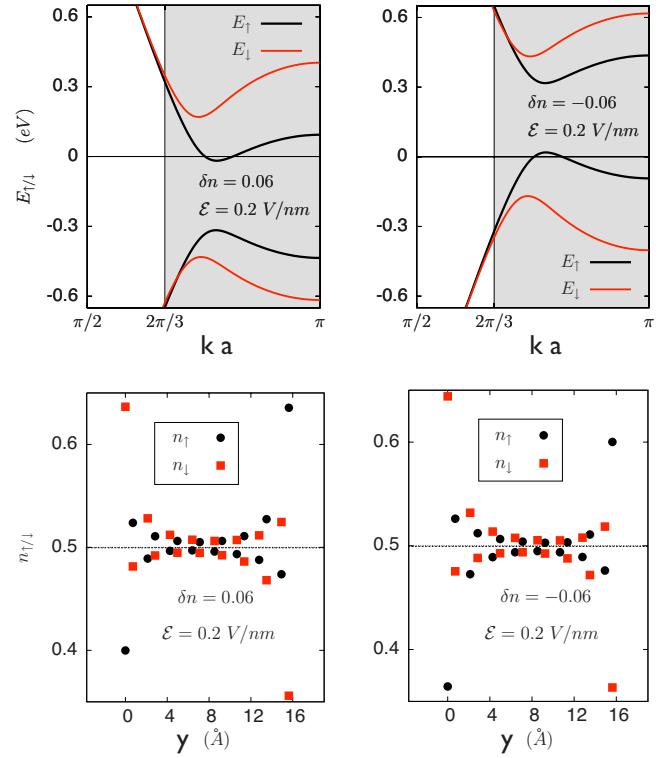


FIG. 5. (Color online) *Top panel*: Band structure of n and p gate-doped $N=8$ zigzag graphene nanoribbons in the presence of a transverse electric field, $\mathcal{E}=0.2$ V/nm, strong enough to produce a collinear $\theta=\pi$ ground state. Note that the edge-state bands are half-metallic in both cases. *Bottom panel*: Spin resolved occupation $n_{\uparrow/\downarrow}(y)$ across the ribbon: majority spin electrons ($\sigma=\uparrow$ for n -doped and $\sigma=\downarrow$ for p -doped) in this figure accumulate on the high potential edge of the ribbon for $\delta n=0.06$ and on the low-potential side for $\delta n=-0.06$.

case a small external magnetic field would be enough to define the easy magnetization axis.

VI. DISCUSSION

Typical results for the edge-state bands of both electron and hole doped zigzag ribbons with a transverse field strong enough to induce the $\theta=\pi$ state are illustrated in Fig. 5. Because of the partial occupation of the highest unoccupied band of the n -doped case and the lowest unoccupied band in the p -doped case, the $\theta=\pi$ state has an overall spin-polarization proportional in magnitude to the doping. Note that these $\theta=\pi$ states are always half-metallic. This ferromagnetic component of the order allows Zeeman coupling from an external magnetic field to fix the spin orientation on each edge. It follows from Fig. 5 that the majority spins are high-energy spins in the n -doped case and low-energy spins in the p -doped case. For a fixed magnetic field direction, the spin-orientations on both edges can therefore be switched with a gate voltage, which changes the sign of the carrier density. This remarkable property of zigzag edge magnetism has no parallel of which we are aware in any other magnetic system.

In closing we remark that the one-dimensional character of zigzag edge magnetism works against robust collective spin properties. As analyzed in more detail elsewhere,^{18,22} the consequences of reduced dimensionality are somewhat mitigated by the substantial stiffness of zigzag edge moments, which are large enough to provide estimates of spin correlation length of the order of a nanometer at room temperature. Nevertheless, robust magnetism in graphitic nanostructures will likely require exchange-coupled two-dimensional ribbon networks. The rather unique properties of

graphitic magnetism discussed in this paper motivate an effort to realize structures of this type.

ACKNOWLEDGMENTS

We acknowledge financial support from the Welch Foundation, NRI-SWAN, the DoE grant (Grant No. DE-FG03-02ER45958, Division of Materials Sciences and Engineering), the Spanish Ministry of Education through the MEC-Fulbright program and Fan Zhang for his help with figures.

*jjeil@physics.utexas.edu

- ¹S. A. Wolf, D. D. Awschalom, R. A. Buhrman, J. M. Daughton, S. von Molnár, M. L. Roukes, A. Y. Chtchelkanova, D. M. Treger *Science* **294**, 1488 (2001); I. Zutic, J. Fabian, and S. Das Sarma, *Rev. Mod. Phys.* **76**, 323 (2004); T. Dietl *et al.*, *Spintronics* (Elsevier, New York, 2008).
- ²D. Awschalom and N. Samarth, *Physics* **2**, 50 (2009).
- ³D. C. Ralph and M. D. Stiles, *J. Magn. Magn. Mater.* **320**, 1190 (2008).
- ⁴J. Akerman, *Science* **308**, 508 (2005).
- ⁵P. Grünberg, *Rev. Mod. Phys.* **80**, 1531 (2008).
- ⁶M. Julliere, *Phys. Lett. A* **54**, 225 (1975); J. Mathon and A. Umerski, *Phys. Rev. B* **63**, 220403(R) (2001).
- ⁷H. Munekata, H. Ohno, S. von Molnar, A. Segmüller, L. L. Chang, and L. Esaki, *Phys. Rev. Lett.* **63**, 1849 (1989); H. Ohno, D. Chiba, F. Matsukura, T. Omiya, E. Abe, T. Dietl, Y. Ohno, and K. Ohtani, *Nature* **408**, 944 (2000); A. H. MacDonald, P. Schiffer, and N. Samarth, *Nat. Mater.* **4**, 195 (2005); T. Jungwirth, J. Sinova, J. Mašek, J. Kučera, A. H. MacDonald, *Rev. Mod. Phys.* **78**, 809 (2006).
- ⁸J. E. Hirsch, *Phys. Rev. Lett.* **83**, 1834 (1999); J. Sinova, D. Culcer, Q. Niu, N. A. Sinitsyn, T. Jungwirth, and A. H. MacDonald, *ibid.* **92**, 126603 (2004); S. Murakami, N. Nagaosa, and S.-C. Zhang, *Science* **301**, 1348 (2003).
- ⁹X.-L. Qi, T. L. Hughes, and S. C. Zhang, *Phys. Rev. B* **78**, 195424 (2008).
- ¹⁰M. Fujita, K. Wakabayashi, K. Nakada, and K. Kusakabe, *J. Phys. Soc. Jpn.* **65**, 1920 (1996).
- ¹¹T. Hikihara, X. Hu, H.-H. Lin, and C.-Y. Mou, *Phys. Rev. B* **68**, 035432 (2003).
- ¹²S. Dutta, S. Lakshmi, and S. K. Pati, *Phys. Rev. B* **77**, 073412 (2008).
- ¹³H. Lee, Y.-W. Son, N. Park, S. Han, and J. Yu, *Phys. Rev. B* **72**, 174431 (2005).
- ¹⁴K.-I. Sasaki, S. Murakami, and R. Saito, *J. Phys. Soc. Jpn.* **75**, 074713 (2006).
- ¹⁵Y.-W. Son Marvin L. Cohen, and Steven G. Louie, *Phys. Rev. Lett.* **97**, 216803 (2006).
- ¹⁶Y.-W. Son Marvin L. Cohen, and Steven G. Louie, *Nature (London)* **444**, 347 (2006).
- ¹⁷L. Pisani, J. A. Chan, B. Montanari, and N. M. Harrison, *Phys. Rev. B* **75**, 064418 (2007).
- ¹⁸O. V. Yazyev and M. I. Katsnelson, *Phys. Rev. Lett.* **100**, 047209 (2008).
- ¹⁹J. Fernández-Rossier, *Phys. Rev. B* **77**, 075430 (2008).
- ²⁰W. Y. Kim and K. S. Kim, *Nat. Nanotechnol.* **3**, 408 (2008).
- ²¹J. Jung, T. Pereg-Barnea, and A. H. MacDonald, *Phys. Rev. Lett.* **102**, 227205 (2009).
- ²²J.-W. Rhim and K. Moon, *Phys. Rev. B* **80**, 155441 (2009).
- ²³S. Bhowmick and V. B. Shenoy, *J. Chem. Phys.* **128**, 244717 (2008).
- ²⁴J. Fernández-Rossier and J. J. Palacios, *Phys. Rev. Lett.* **99**, 177204 (2007).
- ²⁵M. Topsakal, H. Sevincli, and S. Ciraci, *Appl. Phys. Lett.* **92**, 173118 (2008).
- ²⁶W. Yao, S. A. Yang, and Q. Niu, *Phys. Rev. Lett.* **102**, 096801 (2009).
- ²⁷K. Nakada, M. Fujita, G. Dresselhaus, and M. S. Dresselhaus, *Phys. Rev. B* **54**, 17954 (1996).
- ²⁸K. Wakabayashi, M. Fujita, H. Ajiki, and M. Sigrist, *Phys. Rev. B* **59**, 8271 (1999).
- ²⁹M. Ezawa, *Phys. Rev. B* **73**, 045432 (2006).
- ³⁰L. Brey and H. A. Fertig, *Phys. Rev. B* **73**, 235411 (2006).
- ³¹D. Gunlycke, D. A. Areshkin, L. Junwen, J. W. Mintmire, and C. T. White, *Nano Lett.* **7**, 3608 (2007); D. Gunlycke, H. M. Lawler, and C. T. White, *Phys. Rev. B* **75**, 085418 (2007).
- ³²M. Zarea, C. Busser, and N. Sandler, *Phys. Rev. Lett.* **101**, 196804 (2008).
- ³³M. Y. Han, Barbaros Özyilmaz, Y. Zhang, and P. Kim, *Phys. Rev. Lett.* **98**, 206805 (2007).
- ³⁴X. Li, X. Wang, L. Zhang, S. Lee, and H. Dai, *Science* **319**, 1229 (2008).
- ³⁵S. S. Datta, D. R. Strachan, S. M. Khamis, and A. T. C. Johnson, *Nano Lett.* **8**, 1912 (2008).
- ³⁶L. C. Campos, V. R. Manfrinato, J. D. Sanchez-Yamagishi, J. Kong, and P. Jarillo-Herrero, *Nano Lett.* **9**, 2600 (2009).
- ³⁷L. Ci, L. Song, D. Jariwala, A. L. Elías, W. Gao, M. Terrones, and P. M. Ajayan, *Adv. Mater.* **21**, 4487 (2009).
- ³⁸X. Jia, M. Hofmann, V. Meunier, B. G. Sumpter, J. Campos-Delgado, J. M. Romo-Herrera, H. Son, Y.-P. Hsieh, A. Reina, J. Kong, M. Terrones, and M. S. Dresselhaus, *Science* **323**, 1701 (2009).
- ³⁹C. O. Girit, J. C. Meyer, R. Ermi, M. D. Rossell, C. Kisielowski, L. Yang, C.-H. Park, M. F. Crommie, M. L. Cohen, S. G. Louie, and A. Zettl, *Science* **323**, 1705 (2009).
- ⁴⁰A. Chuvilin, J. C. Meyer, G. Algara-Siller, and U. Kaiser, *New J. Phys.* **11**, 083019 (2009).
- ⁴¹J. J. Palacios, J. Fernández-Rossier, and L. Brey, *Phys. Rev. B* **77**, 195428 (2008).
- ⁴²H. Ohldag, T. Tyliczszak, R. Höhne, D. Spemann, P. Esquinazi,

- M. Ungureanu, and T. Butz, *Phys. Rev. Lett.* **98**, 187204 (2007).
- ⁴³O. V. Yazyev, *Phys. Rev. Lett.* **101**, 037203 (2008).
- ⁴⁴J. Jung, T. Pereg-Barnea, and A. H. MacDonald (unpublished).
- ⁴⁵J. S. Cervenka, M. I. Katsnelson, and C. F. J. Flipse, *Nat. Phys.* **5**, 840 (2009).
- ⁴⁶A. H. Castro Neto, F. Guinea, N. M. R. Peres, K. S. Novoselov, and A. K. Geim, *Rev. Mod. Phys.* **81**, 109 (2009); A. K. Geim and K. S. Novoselov, *Nat. Mater.* **6**, 183 (2007); A. K. Geim and A. H. MacDonald, *Phys. Today* **60**(8), 35 (2007).
- ⁴⁷K. Sawada, F. Ishii, M. Saito, S. Okada, and T. Kawai, *Nano Lett.* **9**, 269 (2009).
- ⁴⁸J. Jung and A. H. MacDonald, *Phys. Rev. B* **79**, 235433 (2009).
- ⁴⁹D. S. Novikov, *Phys. Rev. Lett.* **99**, 056802 (2007).
- ⁵⁰E. Rudberg, P. Salek, and Y. Luo, *Nano Lett.* **7**, 2211 (2007).
- ⁵¹E.-J. Kan, Z. Li, J. Yang, and J. G. Hou, *Appl. Phys. Lett.* **91**, 243116 (2007).
- ⁵²H. Min, J. E. Hill, N. A. Sinitsyn, B. R. Sahu, L. Kleinman, and A. H. MacDonald, *Phys. Rev. B* **74**, 165310 (2006).
- ⁵³D. Huertas-Hernando, F. Guinea, and A. Brataas, *Phys. Rev. B* **74**, 155426 (2006).
- ⁵⁴M. Gmitra, S. Konschuh, C. Ertler, C. Ambrosch-Draxl, and J. Fabian, *Phys. Rev. B* **80**, 235431 (2009).